

Crustal seismicity and subduction morphology around Antofagasta, Chile: preliminary results from a microearthquake survey

D. Comte^{a,c}, M. Pardo^{a,c}, L. Dorbath^{b,d}, C. Dorbath^{b,d}, H. Haessler^b, L. Rivera^b,
A. Cisternas^b and L. Ponce^c

^a Departamento de Geología y Geofísica, Universidad de Chile, Casilla 2777, Santiago, Chile

^b Institut de Physique du Globe de Strasbourg, 5 rue Rene Descartes, 67084 Strasbourg Cedex, France

^c Instituto de Geofísica, Universidad Nacional Autónoma de México, México D.F. 04510, México

^d ORSTOM, 213 rue La Fayette, 75480 Paris Cedex 10, France

(Received July 30, 1990; revised version accepted March 5, 1991)

ABSTRACT

Comte, D., Pardo, M., Dorbath, L., Dorbath, C., Haessler, H., Rivera, L., Cisternas, A. and Ponce, L., 1992. Crustal seismicity and subduction morphology around Antofagasta, Chile: preliminary results from a microearthquake survey. In: R.A. Oliver, N. Vatin-Pérignon and G. Laubacher (Editors), *Andean Geodynamics*. *Tectonophysics*, 205: 13–22.

During September–October 1988, 13 analog and 16 digital seismographs were installed in northern Chile within 100 km around the city of Antofagasta (22.5–24.5°S; 68.5–70.5°W). The purposes of this study were to observe the microseismicity, to describe the morphology of the subducting slab near the southern edge of the rupture of the last great 1877 earthquake ($M_w = 8.8$) in the northern Chile seismic gap, and to monitor the seismic activity probably associated with the Atacama fault system that is roughly parallel to the coast.

The analysis of the analog records provides a total of 552 reliable events ($2.0 < M < 5.0$), whose hypocentres delineate the morphology of the subducting plate in the region. The Nazca plate subducts to the east with a dip of 10° along the trench from 22°S to 25°S down to 30 km depth. At 30–60 km depth a slight variation in the dip angle is observed from 17° (22–23.5°S) to 14° (24–25°S). Downplate, from 60 to 100 km in depth, the dip angle increases more rapidly to the north of 23.5°S than to the south of this latitude, where an almost constant dip (14–16°) is observed and the subducting plate becomes more subhorizontal. For greater depths (100–150 km), the dip of the subducting Nazca plate gradually varies from 36° to 18° between 22°S and 24.5°S.

South of 24°S and below 100 km depth, an absence of seismicity is observed. However, a cluster of intermediate depth activity is located near the hypocentre of the December 9, 1950 ($M_w = 8.2$) intraplate normal fault earthquake, around 500 km inland from the trench.

Shallow seismicity (depth ≤ 30 km) is located near the Atacama fault system. Focal mechanisms show normal faulting with slight left-lateral motion along an average strike in the north-northeast–south-southwest direction, which is in agreement with the observed superficial orientation of the fault. Shallow seismicity is also observed on the Mejillones Peninsula, the main irregularity along the coastline. Focal mechanisms of microearthquakes located near the Cerro Moreno fault, which is in the Mejillones Peninsula show left-lateral motion along a north–south fault plane, similar to the fault orientation observed in the field. South of Antofagasta, the Coastal Scarp presents shallow seismicity. Focal mechanisms were possible to obtain only for events with depths between 20 and 30 km which are characterized by thrust faults and are probably associated with the interplate subducting zone.

Introduction

The northern Chile region has been identified as a seismic gap (Kelleher, 1972; Nishenko, 1985)

Correspondence to: D. Comte, Departamento de Geología y Geofísica, Universidad de Chile Casilla 2777, Santiago, Chile.

which is reaching the maturity of its earthquake cycle (Lay et al., 1989; Campos and Comte, 1989; Comte and Pardo, 1991). Hence, the region has a high potential for the occurrence of a great earthquake in the near future.

Historical seismicity indicates that great earthquakes with associated destructive tsunamis have affected the region. The last great event occurred in 1877 with an estimated magnitude of $M_w = 8.8$ and rupture length of 420 km (Comte and Pardo, 1991). The tsunami generated by this earthquake severely damaged major cities along the coastal region.

The studied region around the city of Antofagasta is located near the southern edge of the rupture zone of the great 1877 earthquake. A temporal seismological network of 13 analog and 16 digital seismographs was installed within 100 km around Antofagasta (22.5–24.5°S) with two main purposes: (1) to identify spatial seismic patterns and describe in more detail the poorly known morphology of the subducting slab near the southern limit of the predicted earthquake rupture zone; and (2) to monitor the seismic activity probably associated with the Atacama fault system that roughly parallels the coast in the region.

Several authors have reported changes in the dip angle of the Wadati-Benioff zone in northern Chile. Based on NOAA and ISC hypocentre data,

a segmented subducting Nazca plate with dips varying between 10° and 30° was proposed (Isacks and Molnar, 1971; Swift and Carr, 1974; Barazangi and Isacks, 1976, 1979; Isacks and Barazangi, 1977). Another model postulates a continuous Nazca plate with a dip of about 30° (Sacks, 1977; James, 1978; Snoke et al., 1977, 1979; Hasegawa and Sacks, 1981). A model similar to the one proposed by Hasegawa and Sacks (1981) is obtained by Chowdhury and Whiteman (1987) applying trend surface analysis to represent the subducting lithosphere; the overall shape of the Wadati-Benioff zone appears to be a continuous but undulating slab, rather than separate tongues or a segmented slab.

Data analysis

A network of 29 portable seismographs was installed in northern Chile, 100 km around the city of Antofagasta, during September–October, 1988 (Fig. 1). The location of each station was determined using topographical maps (1 : 50,000); location accuracy is better than 150 m.

Three types of stations were used: (1) thirteen MEQ-800 analog smoked-paper recorders with L4-C (1 Hz) vertical seismometers (Table 1); the amplifications were generally set up to 84 db, corresponding to a magnification of about 5×10^5 at 10 Hz; recording speed was 60 mm/min;

TABLE 1

Analog MEQ-800 station coordinates

Name	Lat. S	Long. W	Elev.	Location
CAL	22°28.81'	69°01.52'	2030	Calama
HOS	22°57.47'	70°16.69'	270	Hornitos
DVM	23°15.05'	70°20.61'	360	Desv. Mejillones
CLB	23°20.37'	69°46.09'	1320	Culebron
MIR	23°21.44'	70°10.60'	1225	Miranda
CHO	23°03.33'	69°35.59'	1570	Chacabuco
FAR	23°29.87'	70°17.92'	950	Farol
CUE	23°37.68'	69°56.31'	960	Cuevitas
COL	23°46.60'	70°26.33'	150	Coloso
TOS	23°54.86'	70°15.51'	720	Tosca
YUG	24°01.23'	69°51.77'	1250	Yugoslavia
YNG	24°05.36'	70°05.14'	1070	Yungay
ROS	24°27.43'	69°53.50'	1470	Rosario

Elevations are in meters relative to the sea level.

records were changed every 48 h and the drift of the internal clock of each instrument was checked at this same interval by direct recording of time pulses transmitted by the WWV station in Colorado, USA or by the LOL station in Argentine; (2) eight digital GEOSTRAS recorders with L22 (2 Hz) three-component seismometers; and (3) a digital telemetric array composed of eight digital stations with L4-C (1 Hz) vertical seismometers; an OMEGA time receiver provided accurate time to each digital station.

This preliminary work presents only the analysis of the smoked-paper records. The accuracy of analog-record readings depends on the level of the background noise and the sharpness of the onsets. On the average, an accuracy of 0.1 s for P arrival onsets is estimated. The S wave onsets were read only when they could be confidently identified: the uncertainty in the S wave arrival time is estimated to be less than ± 0.5 s.

The earthquakes were located using the HYPO71 program (Lee and Lahr, 1978). Arrival

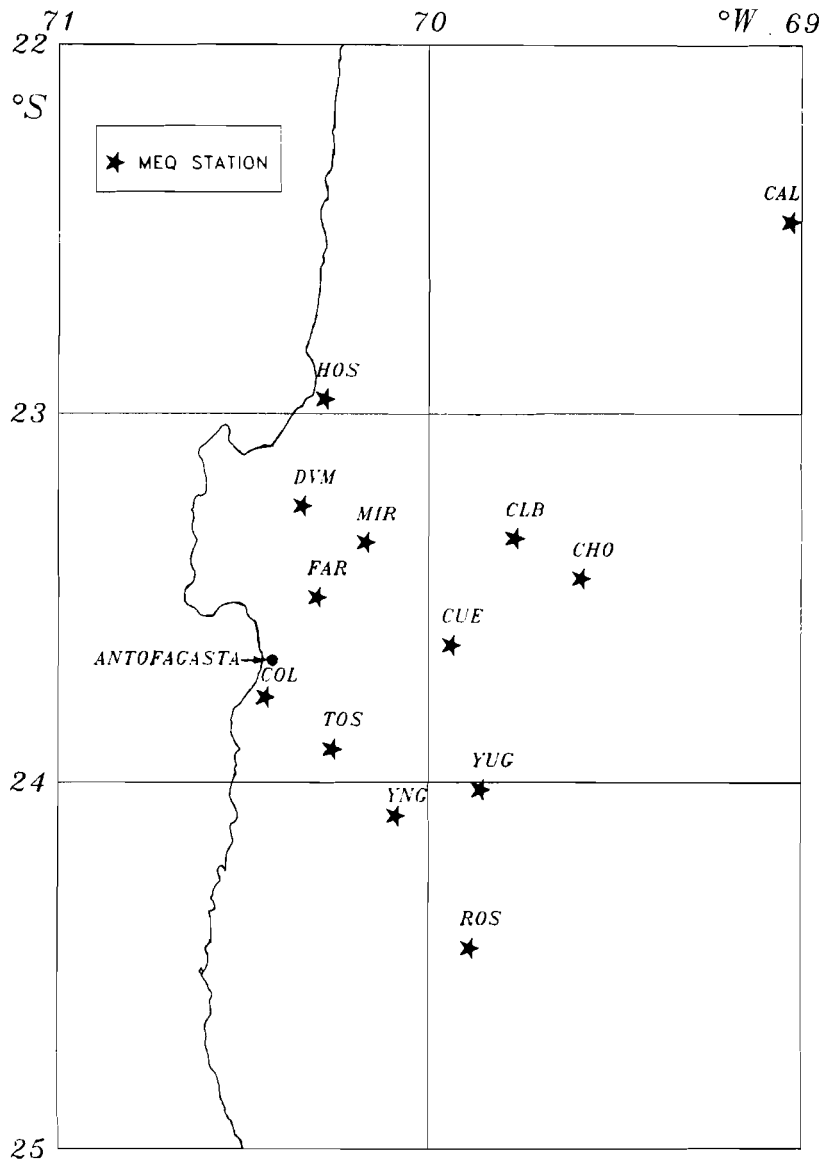


Fig. 1. Sites of the 13 analog temporal seismic stations deployed around the city of Antofagasta during September and October 1988.

TABLE 2

P wave velocity model of the studied zone modified from Wigger (1988), used to locate hypocenters of the recorded events

V_p (km/s)	h (km)
5.5	00.0
6.2	06.0
6.8	10.0
7.2	29.0
8.0	55.0

times showing large residuals were checked and read again if necessary. The assumed P wave velocity model was inferred from the seismic refraction studies in the zone reported by Wigger (1988) (Table 2). The initial depth of HYPO71 was varied every 20 km between 0 and 200 km to evaluate the accuracy of the hypocentral depth determination.

A total of 552 earthquakes with RMS less than 0.5 and duration magnitude from 2.0 to 5.0 were located using a minimum of six arrival times with

at least one S phase (Fig. 2). The epicentres are located in an area of about 300 by 400 km². Most of them are intermediate depth events within the subducting Nazca plate. In addition, 52 shallow events (depth ≤ 30 km) were located, most of them with epicentres near the Atacama fault system and the Coastal Scarp.

Within the area of resolution of the network, 210 events with stable solutions were obtained (Fig. 2). A nearly beltlike arrangement of epicentres is observed: shallow events are mainly near the coastal range and deeper events are located under the Pre-Cordillera (Fig. 3). A similar pattern has also been described in southern Peru in a comparable geodynamic situation (Grange et al., 1984).

Morphology of the subducting plate

The shape of the subducting plate can be determined from hypocentral information (Figs. 2

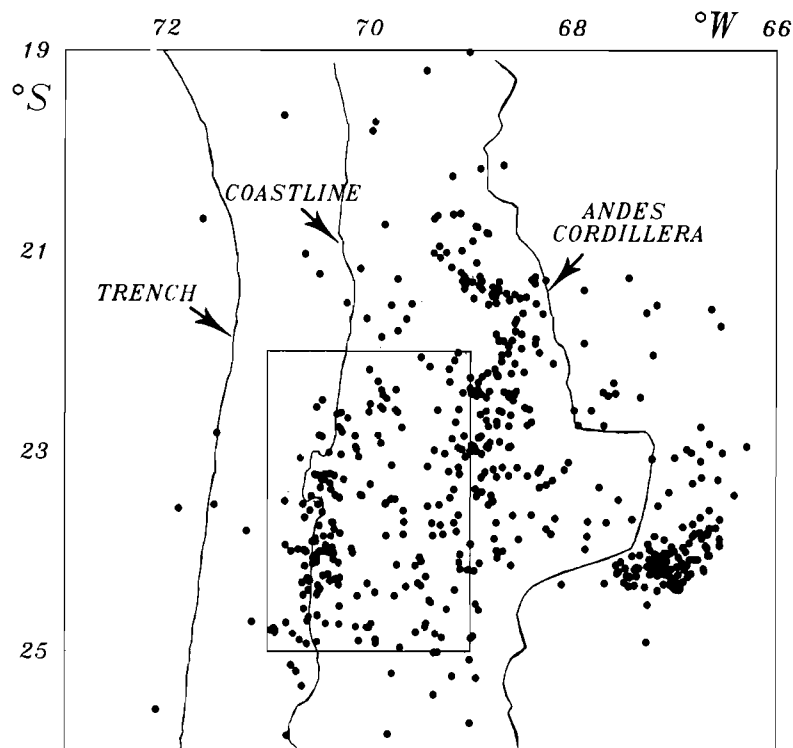


Fig. 2. Epicentres determined using a minimum of six arrival times with at least one S phase and $RMS \leq 0.5$. The rectangle indicates the area of better network coverage. The trench, the coastline and a line that joins the Andes Cordillera summits, which coincides with the Chile border are also shown.

and 3). A set of seven cross-sections normal to the trench were generated every 0.5° between 22°S and 25°S ; each one samples the events within 1° width around the selected latitude (Fig. 4). The cross-sections show a Wadati-Benioff zone dipping in average to the east. The dip angles of segments of the subducting lithosphere were calculated between the depth ranges of 0–30 km, 30–60 km, 60–100 km and 100–150 km and the horizontal distance differences from the trench to these depths along the Wadati-Benioff zone (Table 3, Fig. 4). The dip angle of the subducting slab from the trench to the 30 km depth is ap-

proximately a constant 10° along the region. At 30–60 km depth, the dip increases and a slight variation is observed from 17° ($22\text{--}23.5^\circ\text{S}$) to 14° ($24\text{--}25^\circ\text{S}$). At 60–100 km depth, the dip angle varies from 34° (22°S) to 16° (24.5°S) and at 100–150 km depth changes from 36° (22°S) to 18° (24.5°S). These data suggest that subduction is more horizontal between 23.5°S and 25°S relative to the north of these latitudes.

All proposed models for the subduction in the region (Isacks and Molnar, 1971; Swift and Carr, 1974; Barazangi and Isacks, 1976, 1979; Isacks and Barazangi, 1977; Sacks, 1977; James, 1978;

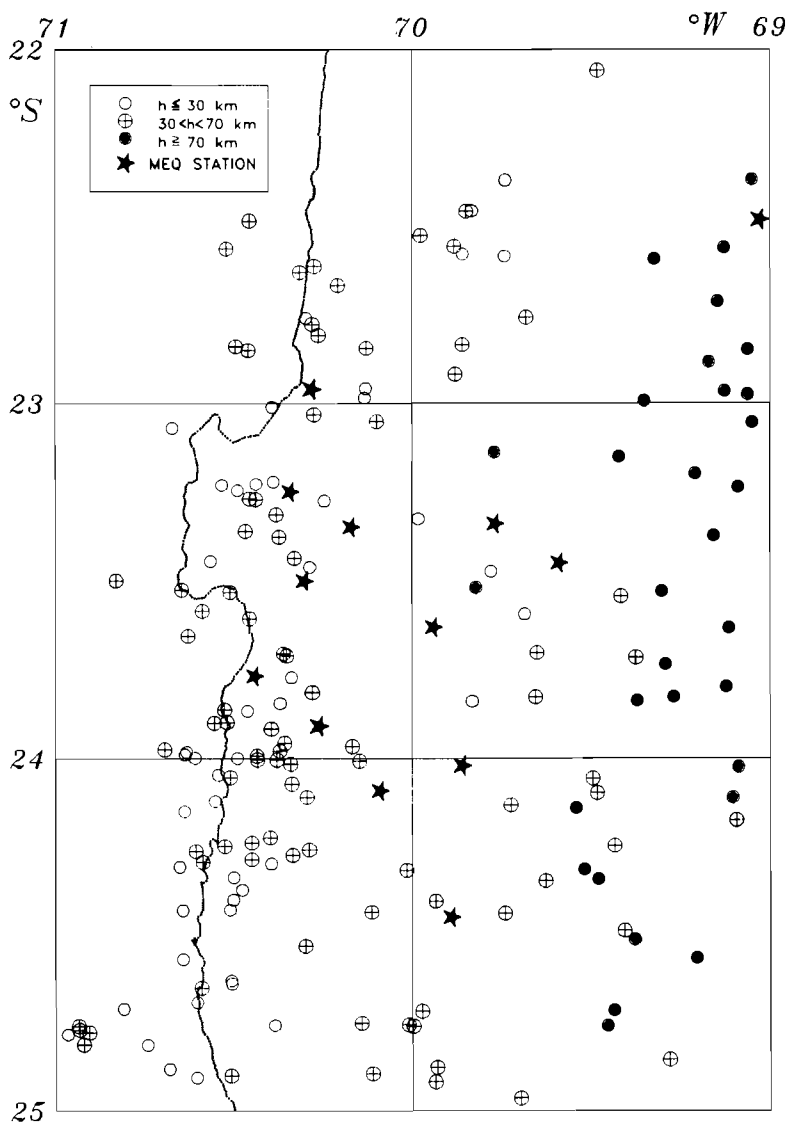


Fig. 3. Map of epicentres of the events with accurate focal depth solutions within the area of the rectangle indicated in Figure 2.

Snoke et al., 1977, 1979; Hasegawa and Sacks, 1981; Chowdhury and Whiteman, 1987) based on teleseismic data indicate that between 19° and 25° S, the dip of the subducting plate is approximately 25° E, which in average agrees with the

observed values determined in the present study at 100 km depth.

The change to a more subhorizontal subduction between 23.5° and 25.0° S is suggested by the seismicity that shows an eastward shift at 100 km

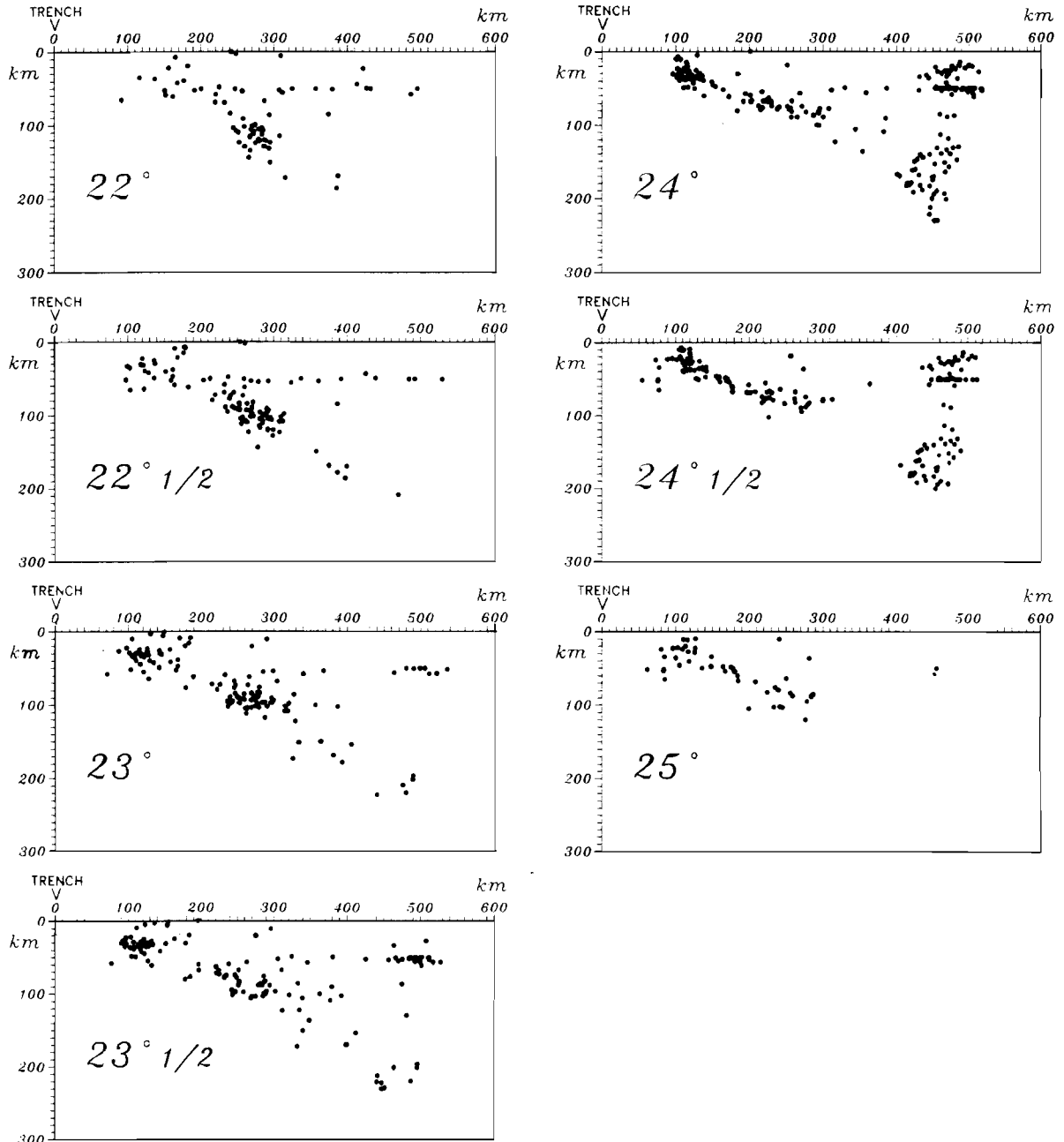


Fig. 4. Cross-sections perpendicular to the trench between 22° and 25° S, including all the events within $\pm 0.5^{\circ}$ around the selected latitude.

TABLE 3

Dip angles of the subducted plate in degrees, for different depths (km) along the plate in each cross-sections of Figure 4 from 22°S to 25°S

Lat. S	30 km	60 km	100 km	150 km
22.0°	[150] 10°	[250] 17°	[310] 34°	[380] 36°
22.5°	[150] 10°	[250] 17°	[310] 34°	[380] 36°
23.0°	[150] 10°	[250] 17°	[330] 27°	[420] 29°
23.5°	[150] 10°	[250] 17°	[360] 20°	[500] 20°
24.0°	[150] 10°	[270] 12°	[410] 16°	[560] 18°
24.5°	[150] 10°	[270] 12°	[410] 16°	[560] 18°
25.0°	[150] 10°	[270] 12°	–	–

Distances from the trench in km are given in brackets.

depth, from 310 km from the trench at 22°S, to 410 km from the trench at 24.5°S. This is well correlated with the eastward bend of the Andes Cordillera and the volcanic axis observed between 22.8° and 24.5°S (Fig. 2).

A cluster of intermediate depth seismicity (150–200 km depth) between latitudes 23.5° and 24.5°S, and 450–500 km from the trench is observed (Fig. 4). A normal fault intraplate earthquake ($M_w = 8.2$) occurred near this zone on December 9, 1950 (Campos, 1989). A region void of microseismicity is observed updip of this cluster. A similar pattern has been observed using teleseismic data (Wigger, 1988; Campos, 1989).

Between 22.5° and 23.5°S, another region void in seismicity is observed at 130–230 km from the trench (60 to 100 km depth), that could indicate the end of the interplate contact between the Nazca and South American plates. To the south, between 23.5° and 25°S, this absence in seismicity is not observed, but an upward slab bending is suggests a higher coupling of the plates.

Northward of 23°S, the interplate seismic activity is scarce in comparison with that observed to the south (Fig. 4). It is interesting to note that this limit corresponds approximately with the southern edge of the seismic gap where the last great earthquake ($M_w = 8.8$) occurred in 1877.

Shallow seismicity

Shallow seismicity (depth ≤ 30 km) is observed at distances from 100 to 200 km from the trench, mainly distributed near the coastline (Figs.

2, 4 and 5). An almost aseismic wedge is present between the trench and the coastline (about 100 km from the trench). Results in other regions suggest that this may be a global phenomenon associated with the presence of weak sediment along the plate boundary (Sacks et al., 1978; Byrne et al., 1988).

Between 22° and 25°S, a correlation of shallow seismicity with the Atacama fault system seems to exist (Fig. 5). Seismicity appears to be more frequent in the vicinity of the fault where branching is prevalent. However, where the fault system consists of a single trace, few shallow microearthquakes were recorded.

Three composite and two single focal mechanisms were determined (Fig. 5). The events near the Salar del Carmen fault show normal faulting with slight left-lateral motion along a trend of north-northeast to south-southwest. This corresponds to the observed strike of the fault recognized in the field (Arabaz, 1971; Armijo and Thiele, 1990).

Shallow seismicity is also observed within the Mejillones Peninsula. Composite focal mechanisms of two microearthquakes located near the Cerro Moreno fault show left-lateral strike-slip motion along a plane striking north–south (Fig. 5), which is the general direction of the Cerro Moreno fault. The sense of left-lateral movement has also been documented by Armijo and Thiele (1990).

Southward of Antofagasta, the shallow events are observed near the branches of the Atacama fault system and the Coastal Scarp (Fig. 5). It was

difficult to obtain reliable first-arrival polarities from the analog seismograms for small shallow events related to the Atacama fault system, so focal mechanisms could not be determined. Seismicity associated with the Coastal Scarp is not observed north of Antofagasta. According to Armijo and Thiele (1990), the Coastal Scarp is a normal fault, but the available data did not allow determination of any focal mechanism. Some deeper events (20–30 km depth) are located beneath the Coastal Scarp. Composite focal mechanisms of two groups of events (left lower side of

Fig. 5) show thrust faulting that might be associated with the subduction of the Nazca plate beneath the South American plate.

Conclusions

The deployment of 13 analog portable seismic stations in northern Chile within 100 km around the city of Antofagasta (22.5–24.5°S; 68.5–70.5°W) during September–October 1988, permits the location of 552 events with duration magnitude ranging from 2.0 to 5.0.

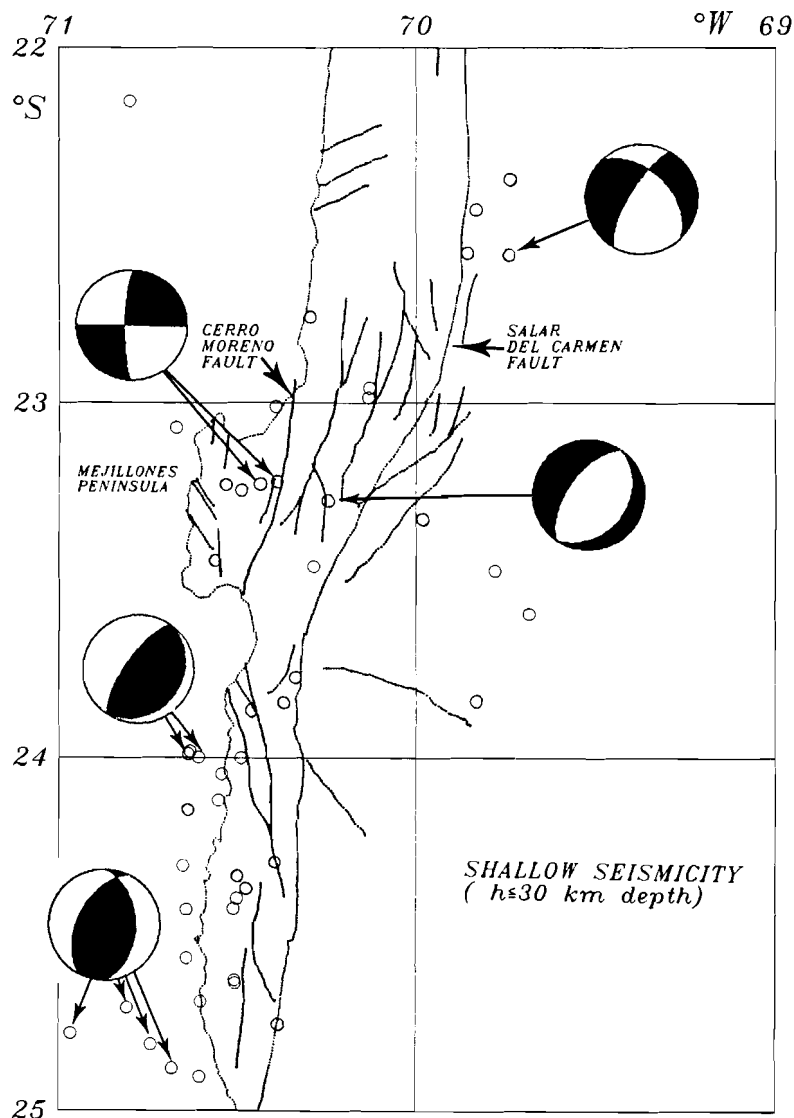


Fig. 5. Shallow seismicity (depth ≤ 30 km) is shown by open circles. The main branches of the Atacama fault system are presented. Composite and single focal mechanisms are projected in the lower hemisphere.

The hypocentres of these events delineate the morphology of the subducting plate in more detail than previous studies using teleseismic NOAA and ISC data, in a zone within or near the southern limit of the rupture of the last great earthquake in northern Chile (1877, $M_w = 8.8$).

From 22°S to 25°S the seismicity indicates that the Nazca plate subducts beneath the South American plate to the east with a dip angle of 10° from the trench down to 30 km depth. At depths greater than 100 km, the dip angle varies from 34° at 22°S to 16° at 24.5°S. South of 23.5°S, the seismicity suggests that from 60 km to 150 km depth, the dip of the plate is almost subhorizontal (14–18°). There is a correlation with the eastward shift of the Andes Cordillera and the volcanic axis in the region.

Between 23.5° and 25°S, a void in seismicity is observed downplate at depths greater than 100 km. However, further east around 500 km from the trench, a cluster of intermediate depth activity is present near the region where the December 9, 1950 ($M_w = 8.2$) intraplate normal fault earthquake occurred.

Shallow seismicity is located close to the Atacama fault system; focal mechanisms show normal faulting with slight left-lateral motion along an average strike of north-northeast to south-southwest in agreement with the orientation of the fault on the surface. Shallow seismicity is also observed near the Cerro Moreno fault in the Mejillones Peninsula with focal mechanisms showing left-lateral motions along a north-south fault plane, which is well correlated with the field observations. Focal mechanisms of shallow coastal seismicity south of Antofagasta show thrust faults, probably associated with the interplate subducting zone.

Acknowledgements

We specially thank Dr. Jacques Deverchere for his invaluable assistance in the field, the staff and students of the Seismological Service of the Department of Geophysics, University of Chile for their collaboration, and the University of Antofagasta for their help in logistics. This work

was supported by ORSTOM, IPG-Strasbourg, University of Chile and by the FONDECYT 1125/89 project.

References

- Arabasz, W.J., 1971. Geological and Geophysical Studies of the Atacama Fault Zone in Northern Chile. Ph.D. thesis, Calif. Inst. Technol., Pasadena, Calif.
- Armijo, R. and Thiele, R., 1990. Active faulting in northern Chile: ramp stacking and lateral decoupling along a subduction plate boundary? *Earth Planet. Sci. Lett.*, 98: 40–61.
- Barazangi, M. and Isacks, B.L., 1976. Spatial distribution of earthquakes and subduction of the Nazca plate beneath South America. *Geology*, 4: 686–692.
- Barazangi, M. and Isacks, B.L., 1979. Subduction of the Nazca plate beneath Peru: evidence from spatial distribution of earthquakes. *Geophys. J.R. Astron. Soc.*, 57: 537–55.
- Byrne, D.E., Davis, D.M. and Sykes, L.R., 1988. Loci and maximum size of thrust earthquakes and the mechanics of the shallow region of the subduction zones. *Tectonics*, 7: 833–857.
- Campos, J., 1989. Determinación de parámetros focales por medio de modelamiento de ondas de cuerpo del sismo del 9 de diciembre de 1950. M.Sci. thesis, Department of Geophysics, University of Chile.
- Campos, J. and Comte, D., 1989. Distribución espacio-temporal del régimen de esfuerzos en el sur del Perú y norte de Chile: ¿evidencias de una etapa de madurez terminal de un ciclo sísmico? *5as Jornadas Chilenas de Sismología e Ingeniería Antisísmica*, 1: 291–302.
- Comte, D. and Pardo, M., 1991. Reappraisal of great historical earthquakes in the northern Chile and southern Peru seismic gaps. *Natural Hazards*, 4: 23–44.
- Chowdhury, D.K. and Whiteman, S.K., 1987. Structure of the Benioff zone under Southern Peru to Central Chile. *Tectonophysics*, 134: 215–226.
- Grange, F., Hatzfeld, D., Cunningham, P., Molnar, P., Roecker, S.W., Suárez, G., Rodríguez, A. and Ocola, L., 1984. Tectonic implications of the microearthquake seismicity and fault plane solutions in southern Peru. *J. Geophys. Res.*, 89: 4971–4980.
- Hasegawa, A. and Sacks, I.S., 1981. Subduction of the Nazca plate beneath Peru as determined from seismic observations. *J. Geophys. Res.*, 86: 4971–4980.
- Isacks, B.L. and Barazangi, M., 1977. Geometry of Benioff zones: lateral segmentation and downward bending of the subducted lithosphere. In: M. Talwani and W. Pitman (Editors), *Island Arcs, Deep Sea Trenches and Back-Arc Basins*. Am. Geophys. Union, Maurice Ewing Ser., 1: 99–114.
- Isacks, B.L. and Molnar, P., 1971. Distribution of stress in the descending lithosphere from a global survey of focal-mechanism solutions of mantle earthquakes. *Rev. Geophys. Space Phys.*, 9: 103–174.

- James, D., 1978. Subduction of the Nazca plate beneath Central Peru. *Geology*, 7: 174–178.
- Kelleher, J.A., 1972. Rupture zones of large South American earthquakes and some predictions. *J. Geophys. Res.*, 77: 2087–2103.
- Lay, T., Astiz, L., Kanamori, H. and Christensen, D.H., 1989. Temporal variation of large intraplate earthquakes in coupled subduction zones. *Phys. Earth Planet. Inter.*, 54: 258–312.
- Lee, W.H.K. and Lahr, J.C., 1978. HYPO71 (Revised): a computer program for determining hypocentre, magnitude, and first motion pattern of local earthquakes. U.S. Geol. Surv. Open-File Rep., 75–311.
- Nishenko, S.P., 1985. Seismic potential for large and great earthquakes along the Chilean and southern Peruvian margins of South America: a quantitative reappraisal. *J. Geophys. Res.*, 90: 3589–3616.
- Sacks, I.S., 1977. Interrelationships between volcanism, seismicity, and anelasticity in Western South America. *J. Geophys. Res.*, 86: 10753–10770.
- Sacks, I.S., Linde, A.T., Rodriguez, A. and Snoke, J.A., 1978. Shallow seismicity in subduction zones. *Geophys. Res. Lett.*, 5: 901–903.
- Snoke, J.A., Sacks, I.S. and Okada, H., 1977. Determination of subducting lithosphere by use of converted phases. *Bull. Seismol. Soc. Am.*, 67: 1051–1060.
- Snoke, J.A., Sacks, I.S. and James, D., 1979. Subductions beneath Western South America: evidence from converted phases. *Geophys. J.R. Astron. Soc.*, 59: 219–225.
- Swift, S.A. and Carr, M.J., 1974. The segmented nature of the Chilean seismic zone. *Phys. Earth Planet. Inter.*, 9: 183–191.
- Wigger, P.J., 1988. Seismicity and crustal structure of the Central Andes. In: *Lecture Notes in Earth Sciences. The Southern Central Andes. Contributions to Structure and Evolution of an Active Continental Margin*. Springer-Verlag, Berlin, pp. 209–227.